

AD-A251 074

(2)



TECHNICAL REPORT BRL-TR-3358

BRL

DEVELOPMENT OF DIAGNOSTICS FOR ELECTROMAGNETIC ARMOR APPLICATIONS

CHARLES R. HUMMER
CLINTON E. HOLLANDSWORTH

JUNE 1992

DTIC
SELECTE
JUN 05 1992
S B D

APPROVED FOR PUBLIC RELEASE; DISTRIBUTION IS UNLIMITED.

U.S. ARMY LABORATORY COMMAND

BALLISTIC RESEARCH LABORATORY
ABERDEEN PROVING GROUND, MARYLAND

92-14642



92 6 03 048

NOTICES

Destroy this report when it is no longer needed. DO NOT return it to the originator.

Additional copies of this report may be obtained from the National Technical Information Service, U.S. Department of Commerce, 5285 Port Royal Road, Springfield, VA 22161.

The findings of this report are not to be construed as an official Department of the Army position, unless so designated by other authorized documents.

The use of trade names or manufacturers' names in this report does not constitute indorsement of any commercial product.

REPORT DOCUMENTATION PAGEForm Approved
OMB No. 0704-0188

Public reporting burden for this collection of information is estimated to average 1 hour per response, including the time for reviewing instructions, searching existing data sources, gathering and maintaining the data needed, and completing and reviewing the collection of information. Send comments regarding this burden estimate or any other aspect of this collection of information, including suggestions for reducing this burden, to Washington Headquarters Services, Directorate for Information Operations and Reports, 1215 Jefferson Davis Highway, Suite 1204, Arlington, VA 22202-4302, and to the Office of Management and Budget, Paperwork Reduction Project (0704-0188), Washington, DC 20503.

1. AGENCY USE ONLY (Leave blank)

2. REPORT DATE

June 1992

3. REPORT TYPE AND DATES COVERED

Final, Apr 1989-Jan 1991

4. TITLE AND SUBTITLE

Development of Diagnostics for Electromagnetic Armor Applications

5. FUNDING NUMBERS

PR: 1L161102AH43

6. AUTHOR(S)

Charles R. Hummer and Clinton E. Hollandsworth

7. PERFORMING ORGANIZATION NAME(S) AND ADDRESS(ES)

8. PERFORMING ORGANIZATION
REPORT NUMBER

9. SPONSORING / MONITORING AGENCY NAME(S) AND ADDRESS(ES)

U.S. Army Ballistic Research Laboratory
ATTN: SLCBR-DD-T
Aberdeen Proving Ground, MD 21005-506610. SPONSORING / MONITORING
AGENCY REPORT NUMBER

BRL-TR-3358

11. SUPPLEMENTARY NOTES

12a. DISTRIBUTION / AVAILABILITY STATEMENT

Approved for public release; distribution is unlimited.

12b. DISTRIBUTION CODE

13. ABSTRACT (Maximum 200 words)

A test stand consisting of an electrified-plate assembly coupled to a small capacitor bank has been assembled, tested, and used to develop diagnostic instrumentation to be exploited in future range experiments in the general area of electromagnetic technology applied to terminal ballistics. A 1.2-m-long air gun is used to propel a length of copper wire through small holes in the electrified-plate assembly to simulate the switch-closure action important to some planned range experiments. Instrumentation to measure the relevant currents and voltages was developed and used to characterize the switch-closing action. The test stand was used to calibrate the diagnostics, test their immunity to noise, and measure their time response. The velocity of the wire was determined by optical means. Using this velocity, the features observed with the diagnostics were then correlated with the position of the wire in the test stand.

14. SUBJECT TERMS

magnetic fields, magnetic forces, air guns

15. NUMBER OF PAGES

33

16. PRICE CODE

17. SECURITY CLASSIFICATION
OF REPORT

UNCLASSIFIED

18. SECURITY CLASSIFICATION
OF THIS PAGE

UNCLASSIFIED

19. SECURITY CLASSIFICATION
OF ABSTRACT

UNCLASSIFIED

20. LIMITATION OF ABSTRACT

SAR

INTENTIONALLY LEFT BLANK.

TABLE OF CONTENTS

	<u>Page</u>
LIST OF FIGURES	v
ACKNOWLEDGMENTS	vii
1. INTRODUCTION	1
2. INSTRUMENTATION AND EXPERIMENT	2
2.1 Air Gun and Sabot	2
2.2 Instrumentation for Velocity Measurement	4
2.3 Parallel Plates and Capacitor Bank Arrangement	4
2.4 Current Measurement Techniques	4
2.5 Voltage Measurement Technique	6
3. EXPERIMENTAL RESULTS	7
3.1 Velocity Measurements	7
3.2 Capacitor Bank Current Measurement	9
3.3 Arc Voltage Measurement	13
4. SUMMARY	15
5. REFERENCES	17
APPENDIX A: PHOTO DETECTION SYSTEM CIRCUITRY	19
APPENDIX B: ROGOWSKI COILS FOR CURRENT MEASUREMENTS	25
DISTRIBUTION LIST	31

INTENTIONALLY LEFT BLANK.

LIST OF FIGURES

<u>Figure</u>		<u>Page</u>
1.	A Sabot for the Air Gun to Launch a Copper Wire	3
2.	Plate Assembly	3
3.	Schematic of the Capacitor Bank	5
4.	Light Path Signals	8
5.	The Time Derivative of the Current for Each Coil	10
6.	The Time Derivative of the Plate Current	11
7.	The Current for Each Coil	11
8.	The Plate Current	12
9.	The Time Derivative of the Electric Field	14
10.	The Plate Voltage	14
A-1.	Self-Biasing PIN Diode Amplifier	22
B-1.	Rogowski Coil in a Toroidal Housing	28



Accession For	
NTIS GRA&I	<input checked="" type="checkbox"/>
DTIC TAB	<input type="checkbox"/>
Unannounced	<input type="checkbox"/>
Justification	
By _____	
Distribution/	
Availability Codes	
Dist	Avail and/or Special
A-1	

INTENTIONALLY LEFT BLANK.

ACKNOWLEDGMENTS

The authors wishes to thank Dr. G. Filby and Mr. E. Rapacki for the air gun and their help in its use. Mr. J. Correrri and Mr. K. Mahan prepared the facilities for the air gun, the capacitor bank, and the data acquisition equipment. Mr. A. Zielinski provided the capacitors and power supply, assisted in calibrating the Rogowski coils, and made several helpful suggestions. Mr. H. Burden and Dr. K. White helped with the editing of the paper.

INTENTIONALLY LEFT BLANK.

1. INTRODUCTION

In 1973, Walker suggested that the metallic jet formed by a shaped charge could be defeated by passing a large electrical current through the jet (Walker 1973). Conceptually, the simplest defeat mechanism is vaporization of the jet, but this process requires an enormous expenditure of electrical energy which, in turn, imposes a significant size and weight burden on any practical system. A number of possible, more efficient electromagnetic (EM) disruption mechanisms, such as the excitation of hydrodynamic instabilities have been suggested. The effects of large, externally supplied electrical currents on the stability properties of copper shaped charge jets have been examined in recent theoretical work at the Ballistic Research Laboratory (BRL) (Powell and Littlefield 1990; Littlefield and Powell 1990).

Advances in pulsed-power technology since the time of Walker's suggestion make it feasible to study experimentally the disruption of shaped charged jets by electromagnetic means. In recent years, proof-of-principle (POP) experiments were conducted by Johnson and Toepfer (1985) and Lim and Cayere (1988), the latter under contract jointly to BRL and the Defense Nuclear Agency (DNA). The present work was done in preparation of future experiments that will further elucidate the defeat mechanisms.

In one possible EM armor design, an outer hull would serve as the electrical ground plate, while an inner, insulated hull would be held at a high potential by a charged capacitor bank, the source of the electrical energy to disrupt the jet. When a shaped charge jet penetrates the ground plate and reaches the "hot" or high-potential plate, it completes a circuit between the plates, connecting the stored energy (power supply) to the plates. Thus, the pulsed-power source in EM armor experiments is fundamentally different from the normal capacitor-bank power supply. In the latter, internal switches within the power supply deliver the stored energy to the load on command, whereas in EM armor experiments the jet from a shaped charge acts as the switch.

A convenient way to simulate the switching action of the jet for bench-top experiments is to use an air or gas gun to propel a copper wire through an electrified-plate assembly. In this report, we describe the development of a laboratory test facility consisting of an

electrified-plate assembly coupled to an existing BRL air gun. The purpose of this effort is to provide both a suitable test stand for use in the development of diagnostics for range experiments planned in succeeding years and a means of developing special techniques for application to EM armor and other EM technology experiments.

2. INSTRUMENTATION AND EXPERIMENT

2.1 Air Gun and Sabot. A 1.2-m air gun with a 2.54-cm bore was used to launch copper wires with diameters of 2.5 mm. Thus, the wires had to be mounted in a carrier to keep the wire centered in the bore and to form a gas seal with the bore. The carrier (Figure 1) developed for these experiments has three parts: (1) a plexiglass front support, (2) a stainless steel thin-wall tube (7.5 cm long and 1.3-cm outside diameter), and (3) a nylon back support. The plexiglass front support is a disk with a hole through the center that is large enough for the copper wire to slip through. The nylon back support has a blind hole at its center to hold the end of the copper wire. On the backside of the plexiglass disk is a flange into which the outside diameter of the stainless steel tube is press-fitted. The nylon back support also has a seat for the stainless steel tube. The diameter of the supports allows a 0.3-mm clearance with the bore. This clearance permits the supports to slide down the bore with minimal resistance while maintaining a gas seal. Thus, the supports center the axis of the stainless steel tube and the copper wire onto the axis of the bore of the air gun.

After the carrier and the wire exit the muzzle of the air gun, the carrier is stopped by a stripper plate (Figure 2). The stripper plate is a 2.54-cm-thick aluminum plate, 20 cm wide and 40 cm tall with a 0.95-cm hole to permit passage of the copper wire. These dimensions give the plate sufficient mass to absorb the momentum of the carrier. Occasionally, in early shots, the stainless steel tube would hit the wire as the tube impacted the stripper plate. This was prevented by placing a steel cone insert with a knife edge in the plate hole. After the plexiglass front support is shattered, the knife edge engages the inside of the tube and splits the tube from the inside, thus directing the tube wall away from the wire.

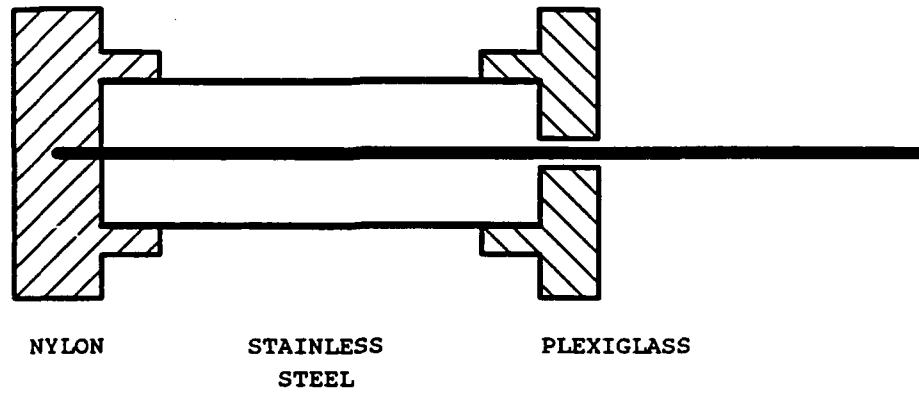


Figure 1. A Sabot for the Air Gun to Launch a Copper Wire.

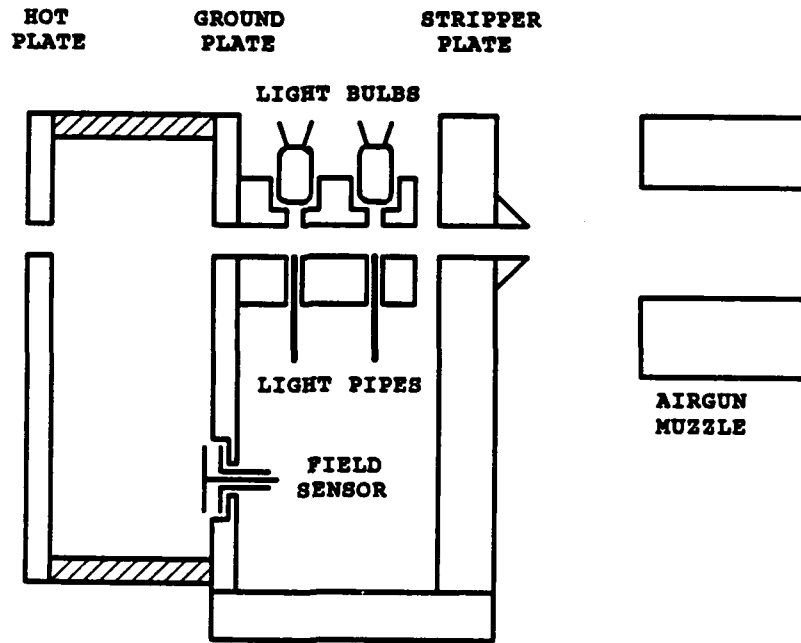


Figure 2. Plate Assembly.

2.2 Instrumentation for Velocity Measurement. After separation from the carrier, the wire intersects two light paths to permit a determination of its velocity. These light paths are located near the entrance to the parallel-plate array, which is connected to a capacitor bank. Electronic circuitry in this region would be very close to large electrical currents and exposed to possible electrical arcs. To avoid this difficulty, light pipes, positioned normal to the trajectory of the wire and opposite a light source, are used to transmit the optical signals to photodetectors located in a well-shielded box at a distance from the parallel plates. The circuitry of the photo detection system is described in Appendix A.

2.3 Parallel Plates and Capacitor Bank Arrangement. The wire enters the parallel plates through a 2.54-cm hole in the first plate which is grounded (Figure 3). The other parallel plate is mounted 5.08 cm from the grounded plate and is connected to the capacitor bank. The wire exits the hot plate through another 2.54-cm hole and is stopped in a catcher box (not shown). The entrance hole and the exit hole are covered with thin, copper tape to serve as electrical connections between the plate and the copper wire while the wire is bridging the gap, and to assist in the initiation of the two arcs, one in each 2.54-cm hole, which are a necessary part of the conduction path for the wire.

The capacitor bank consists of four 500- μ F, 10-kV capacitors, each of which is connected in series with a 35- μ H coil. The four capacitor-coil assemblies are each connected in parallel across the plates (Figure 3). A dump resistor in series with a remote-controlled relay is also connected to the hot plate. When the remote-controlled relay is opened, the hot plate is isolated and the capacitors can then be charged through the coils by the high-voltage power supply. If the charge on the capacitors is to be dumped when a run is aborted or residual charge on the capacitors is to be dumped after the run, the relay is closed, placing the dump resistor directly across the hot plate and ground.

2.4 Current Measurements Techniques. The circuit currents for each capacitor-coil array (see Figure 3) may be obtained from measurements with either current transformers, which measure the current as a function of time, or Rogowski coils, which, if designed properly, can provide voltages proportional to the time derivative of the current threading the loop of the coil. The latter method was chosen for the present experiments because it is more useful in identifying features in the data. In the present experiments, some abrupt changes in circuit

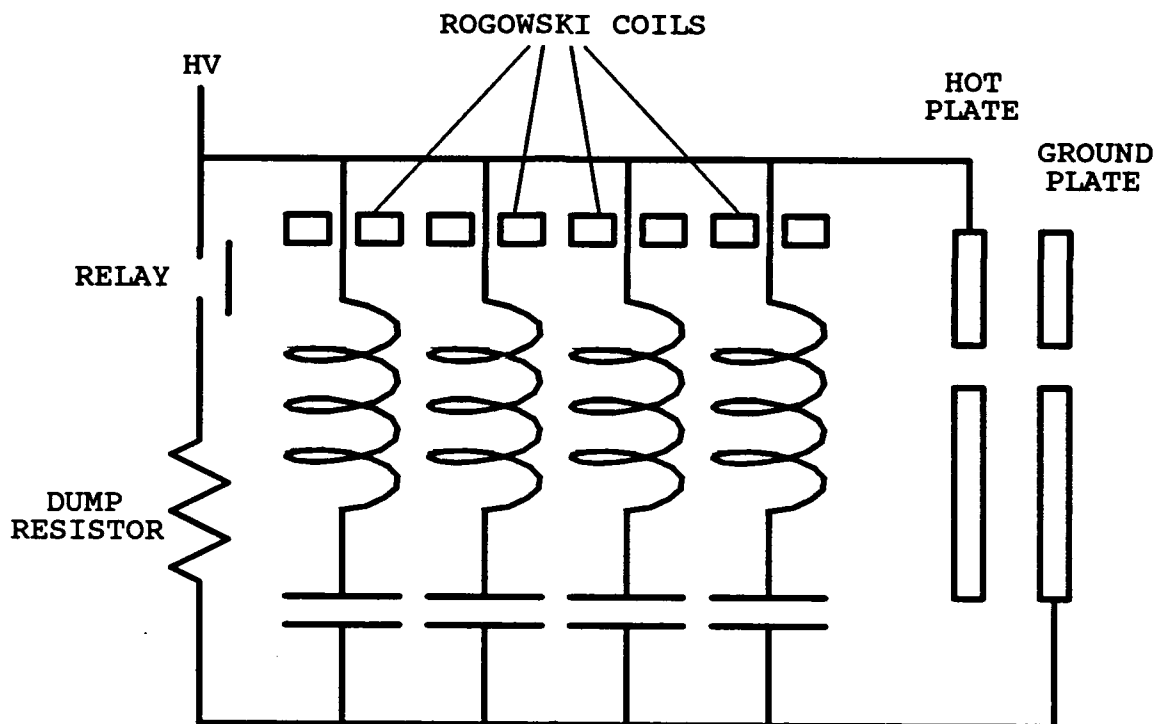


Figure 3. Schematic of the Capacitor Bank.

element parameters not apparent in either the voltage or current waveforms are easily recognizable in waveforms proportional to the derivative of these quantities (see Section 3).

Four Rogowski coils with toroidal cross sections were constructed in the course of this work. The design of these non-integrating Rogowski coils is described in Appendix B. The coils were calibrated against a standard Rogowski coil by placing them all on the same current-carrying cable. The current source was a capacitor bank equipped with an ignitron switch. The signal from each coil was simultaneously recorded by a Nicolet 4094C digital oscilloscope. The wave forms from the four new coils were nearly identical to the standard coil, except for a scaling factor. The sensitivity of each coil was determined by comparison of the peak voltage in the oscilloscope trace for the coil and that for the standard Rogowski coil previously calibrated with a Pearson current-shunt. All four coils were found to have sensitivities within 10% of the desired value. As a further check for consistency, the inductance and internal resistance of each coil was measured with a Hewlett/Packard Model 4274A Multi-Frequency LRC meter, and this result was used to calculate the coil sensitivity using the formulas given in Appendix B. These calculated values also agreed with the

measured ones to within 10%. Measurements of fast-rise time currents from a signal generator indicate that the time response for each coil is about 1.0 μ s, more than adequate for the present experiments.

2.5 Voltage Measurement Technique. To determine the power dissipated by the arc, both the current through the arc and the voltage across the arc must be measured. The conventional way to measure the voltage is to use a voltage divider consisting of a string of resistors. This may not be practical in this experiment for two reasons. First, since the plates must sustain a potential difference for some time before the experiment begins (the copper wire acts as the closing switch which initiates current flow), the resistors would heat up during this time and the calibration might change. Second, the resistor divider presents a load to the charging circuit and capacitor bank. Thus, a voltage sensor that does not present a direct current load is desirable. A sensor that detects the electric field between the plates has this property.

The electric field sensor developed for these experiments (Figure 2) is a 2.5-cm x 7.5-cm section of double-clad circuit board. The front side of the circuit board facing the hot plate is connected to the center conductor of a coaxial cable, and the backside facing the ground plate is connected to the braiding of the coaxial cable. The circuit board is mounted in a recess of the ground plate (as shown in Figure 2) with a fiberglass board to insulate the back face from the ground plate. Also, the front face of the circuit board is covered by a fiberglass board to prevent charged particles from hitting the front side.

When voltage is applied to the hot plate, a charge is induced on the front face of the circuit board. If the charge on the hot plate changes, the amount of induced charge must also change when the sensor front plate is connected to ground through a resistor. Thus, the rate of change of induced charge on the front face is proportional to the center conductor current, which is consequently proportional to the rate of change of the electric field between the plates.

The sensor was calibrated by connecting a high-voltage pulser to the hot plate after disconnecting the capacitor bank. Since this sensor responds to the time derivative of the

voltage across the plates, its signal was recorded, integrated, and compared with plate voltage as measured by a standard resistance voltage-divider.

It was thought that having the back plane insulated from the ground plate would prevent a ground loop that could change the response of the sensor. Calibrations were performed with the sensor back face grounded to the ground plate and then insulated from the ground plate. No significant differences were observed. It was noted, however, that the calibration varied from day to day. Some possible reasons for the variation are changes in humidity, temperature, or the surface conditions of either the copper cladding or the fiberglass boards. However, the variation in the calibration was small, typically of the order of 10%, over a period of hours. Thus, the sensor should be calibrated just prior to a shot.

3. EXPERIMENTAL RESULTS

The experimental data reported herein were recorded on Nicolet 4094C digital oscilloscopes. For each shot, the two light pipe signals, a Rogowski current trace from each of the four LC circuit arrays, and a signal from an electrical-field sensor used to determine the voltage across the plates, were recorded. For some runs, a signal derived from a Rogowski Belt surrounding the support for the ground plate, which sensed the total current in the experiment, was recorded.

3.1 Velocity Measurements. Figure 4 shows the light pipe signals from a typical shot. The top trace, displaced upwards for illustration, is from the light path closest to the air gun. As noted earlier, the arrival of the wire at the light path is indicated by an increase in voltage. Although the rise time of the light detection system is only 0.5 μs , the rise time of the signals in Figure 4 is about 20 μs . Part of this increase is due to the time required for the wire to cross the width of the light path, which is 1.5 mm. For the typical wire velocities used in this experiment, about 20,000 cm/s, this contribution to the rise time should be about 7 μs .

A major contributor to the total rise time observed in the recorded signal is the capacitance of the unterminated coaxial cable used to couple the photodetector output to the waveform recorder which is operated in a high-impedance mode (to keep the remote light detector simple, the amplifiers are very low-power units not capable of driving low-impedance loads

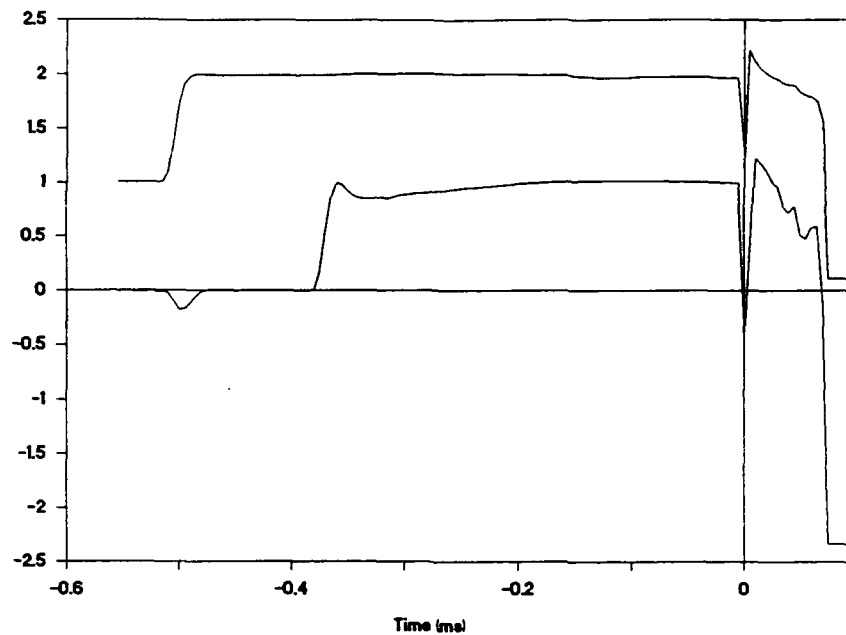


Figure 4. Light Path Signals.

such as terminated coaxial cables). This does not, however, introduce a large uncertainty into the determination of the wire velocity. This contribution to the uncertainty is reduced by taking the arrival time to be the midpoint between the maximum level and the initial level of the signal. Using this criterion, the time for the wire to cross the two light paths (Figure 4) is $131 \mu\text{s}$. With a light path separation of 2.54 cm, the velocity of the wire was determined to be 19,400 cm/s. The initial and maximum signal levels were not distinct, but using different maximum and initial levels did not change the results by more than 700 cm/s. This contribution represents the major uncertainty in the velocity measurement.

There are other features in the light pipe signals. One is a sharp peak at 0.0 ms (see Figure 4) that is present in both light pipe signals. These peaks occur at the time of initial current flow between the plates and may be caused by electrical noise induced by the capacitor bank. Another feature is a sudden drop in the signal at 0.065 ms, which suggests that the PIN diodes received a sudden pulse of light at this time. Because the electrical arc between the plates is a source of very intense light, it is possible that the PIN diodes are responding to reflected light from this source.

Using the measured velocity for the wire, 19,400 cm/s, the time for four important events can be discussed. These events are (1) the wire crossing the light path closest to the muzzle of the air gun, (2) the front end of the wire reaching the hot plate which initiates a current between the plates, (3) the back end of the wire passing the ground plate, and (4) the back end of the wire passing the hot plate. The time of the second event is taken to occur at the origin in Figure 4. This event is marked by a sudden increase of the Rogowski coil signal which monitors the current from the capacitor bank to the plates (Figure 5). Using this time origin, the wire crossed the first light path at $-508 \mu\text{s}$, as determined directly from the data. Since the wire is 15.24 cm long and the spacing between the plates is 5.08 cm, the back end of the wire would be 10.16 cm behind the ground plate when the front tip is at the hot plate. Thus, using the value determined for the velocity of the wire, the back end of the wire should leave the ground plate at $528 \mu\text{s}$ —the time for the third event. Finally, the back end of the wire should leave the hot plate at $792 \mu\text{s}$ —the time for the fourth event. The second and fourth events are manifested in the time derivative of the current between the plates.

The velocity of the wire can be independently determined by measuring the distance between the first light path and the hot plate (10.04 cm) and the time for the first event ($-508 \mu\text{s}$). According to these measurements, the velocity of the wire is 19,800 cm/s. This is 3% larger than the value determined by using the two light pipe signals. With the time relationships established by these optical data, it is possible to relate the significant features in the current traces to the position of the wire in the plate assembly. These correlations are discussed in the following sections.

3.2 Capacitor Bank Current Measurement. When the wire reaches the hot plate and completes the circuit, the currents immediately begin to flow and the time derivative of the current is a maximum. Thus, the signal from the Rogowski coils (Figure 5) rises very quickly to a maximum when the wire completes the circuit, which marks the time for the second event. The time for this event, as stated earlier, is defined as zero. The Rogowski coils show that the current was changing after the third event at $528 \mu\text{s}$ and until the fourth event at $792 \mu\text{s}$. This is the period when the back end of the wire was between the plates. Thus, the current had to flow from the back end of the wire across an air gap whose length was increasing during this period. As the wire left the plates at $792 \mu\text{s}$, the time derivative of the currents dropped to zero when the current between the plates stopped (see Figure 5).

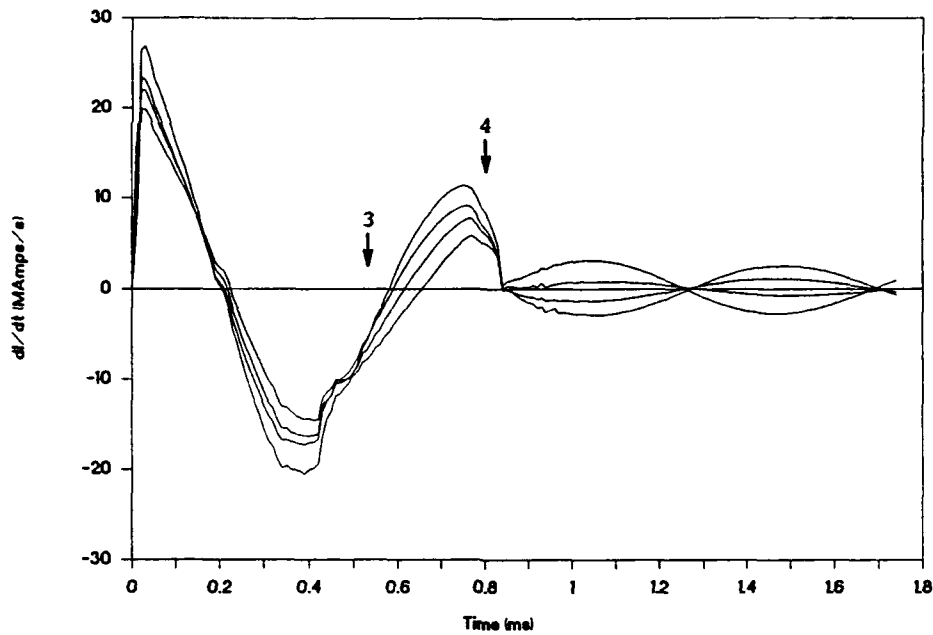


Figure 5. The Time Derivative of the Current for Each Coil.

The Rogowski outputs show that currents flowed through the capacitors after the wire had left the plates entirely. These currents were not flowing through an arc but from one capacitor to another. This can be demonstrated by summing all the Rogowski currents to find the time derivative of the total current between the plates (Figure 6). The result shows that the time derivative of the plate current was zero after the wire had left the plates, or that the current was constant. The plate current itself can be found by numerically integrating the time derivative for each coil to get the current for each coil (Figure 7) and then adding the currents (Figure 8). The results show that the plate current was small, consistent with a value of zero, after the wire exited the plates.

Because current was flowing between the plates, the only other paths that currents could follow were from one capacitor to another. This is possible if the voltages of the capacitors are not all equal after the plate-current flow ceases. Since neither the capacitance nor the inductance of the four circuits are exactly equal, the time dependence of the currents (Figure 7) are not the same. Therefore, the voltages on the capacitors will not be equal when the plate-current flow ceases, and current flow will persist until equalization occurs.

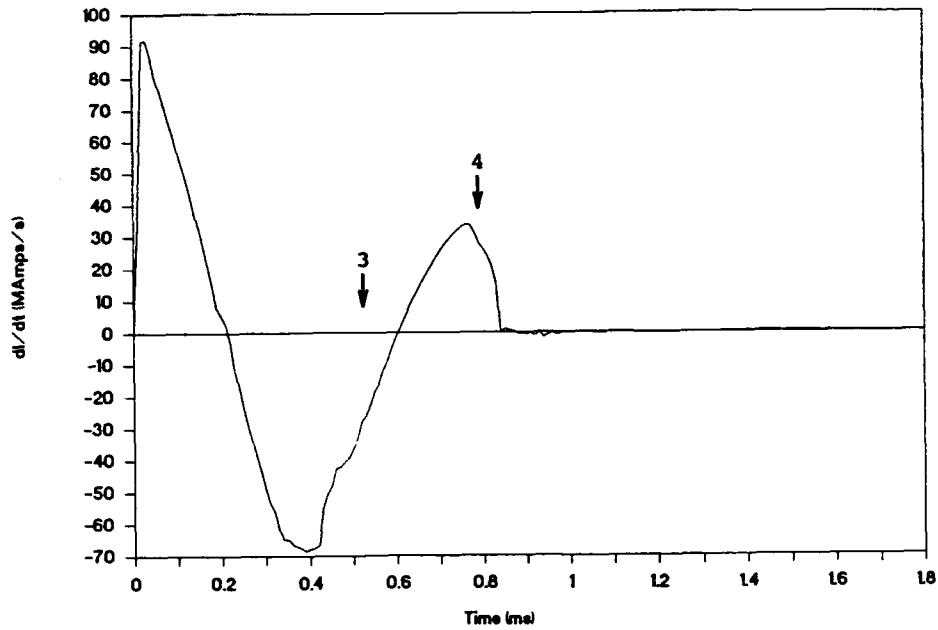


Figure 6. The Time Derivative of the Plate Current.

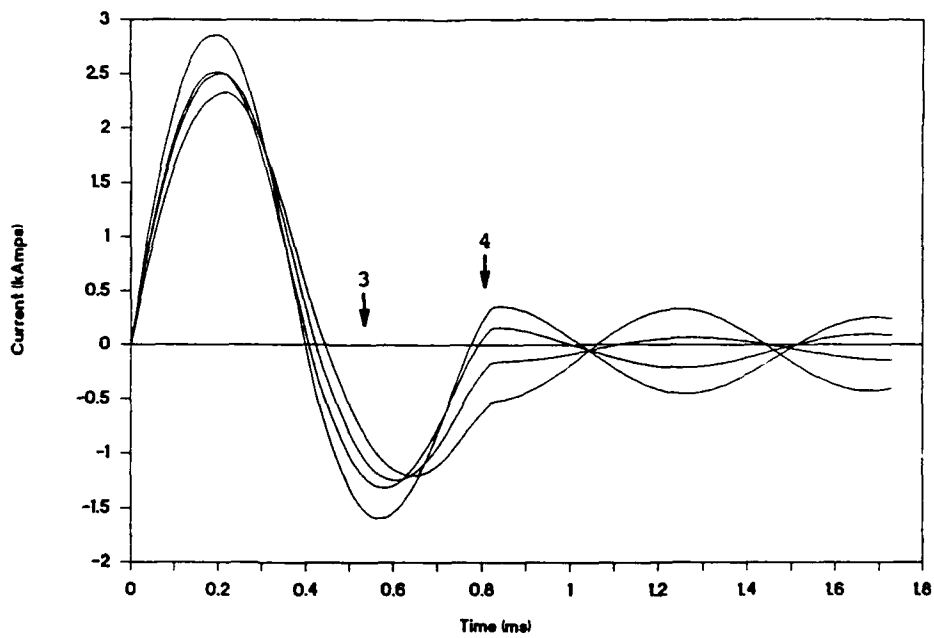


Figure 7. The Current for Each Coil.

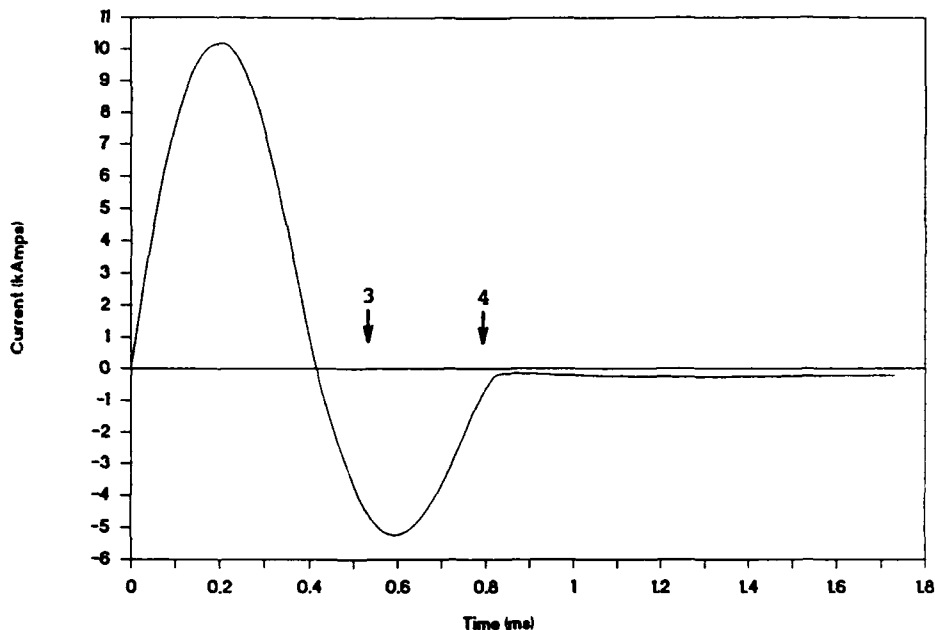


Figure 8. The Plate Current.

The circuit composed of the four capacitors and inductors of the capacitor bank and the arc resistance (Figure 3) can be approximated by an LRC circuit, which consists of an equivalent capacitor, inductor, and resistor connected in series. In our case, the equivalent capacitance ($522 \mu\text{F}$) and inductance ($32 \mu\text{H}$) are estimated by taking the average of the circuit capacitances and inductances, respectively. These estimates are valid when the component values for the four circuits are about equal. The equivalent resistance is equal to the load resistance of the capacitor bank, which is estimated from the decay of the current to be about 0.1 ohms. The total current of the capacitor bank as a function of time can be calculated by using this LRC circuit description, and taking the initial voltage of the capacitor to be four times the voltage of the capacitor bank. With an assumed initial voltage of 3,200 V (the capacitor bank was charged to 800 V) and the equations for a series LRC circuit, the total peak current is calculated to be 10.2 kA at 180 μs returning to zero at 420 μs . These calculated points agree well with the measured current (see Figure 8).

There are rapid changes in the current due to the effects of breakdown in the gas at 420 μs and 830 μs , times when the total current is zero and the direction of the current reverses. When the current approaches zero, the voltage across the arc also approaches

zero. At some time, the voltage will become less than the minimum voltage needed to sustain the arc (Cobine 1941). When the arc current stops, the voltage as supplied by the external circuit can then change rapidly, since the circuit is open. If the supply voltage again becomes larger than the breakdown voltage, the arc will be reestablished. Therefore, the arc voltage is expected to change rapidly when the current crosses zero. In the following section, an indirect method for estimation of the arc voltage is described. This method is particularly sensitive to small changes in the condition of the arc.

3.3 Arc Voltage Measurement. The signal from the electric-field sensor for a typical wire shot is shown in Figure 9. When the arc starts at zero time, the plate voltage changes from 800 V, the capacitor-bank voltage, to approximately 0.0 V (Figure 10). This means that the time derivative of the plate voltage is very large; indeed, the signal at zero time is saturated. The two other major peaks mark when the arc current passes through zero and reverses direction.

The arc voltage (V) can be calculated from the time derivative of the current, as measured by the Rogowski coil in the loop, by using the circuit equation

$$V = Q/C - L \, di/dt .$$

The quantity (Q) is the charge on one of the capacitors (C) in the bank, and di/dt is the time derivative of the current through the inductor (L) connected to that capacitor. The only quantity that is not known or directly measured in this equation is the charge on the capacitor. The charge, however, can be derived by integrating di/dt twice—once to obtain the current and again to obtain the charge. The result of this calculation is shown as a solid line in Figure 10.

Integration of the signal from the electric-field sensor and the addition of a constant offset voltage produces a curve (the pluses in Figure 10) which is in qualitative agreement with the plate voltage determined by integration of the Rogowski traces. The poor agreement at early times is to be expected due to the fact that the sensor signal saturates the amplifier, and the recovery time for the circuit is time dependent and uncertain. The sensor data are, however, in good qualitative agreement with the plate voltage determined by other means.

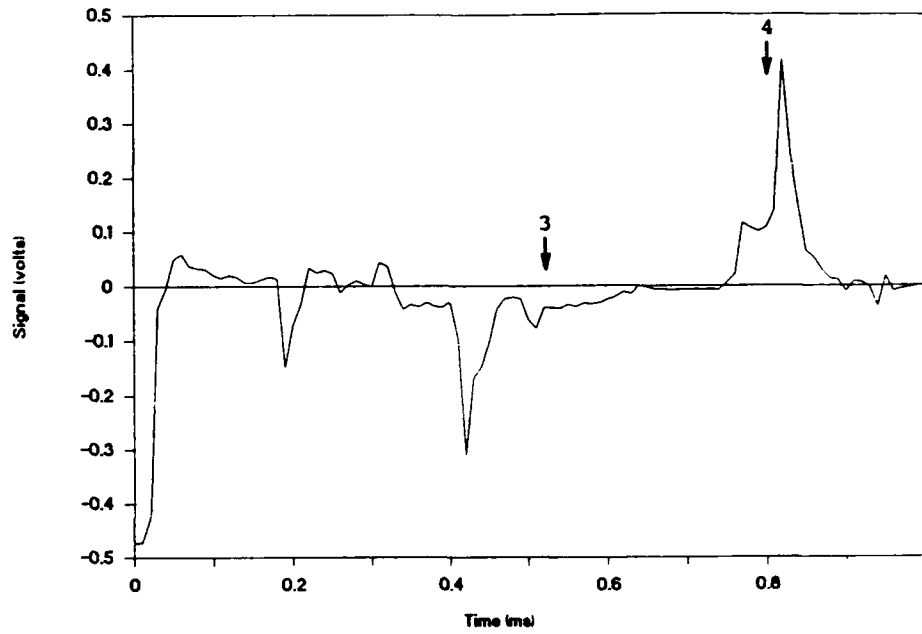


Figure 9. The Time Derivative of the Electric Field.

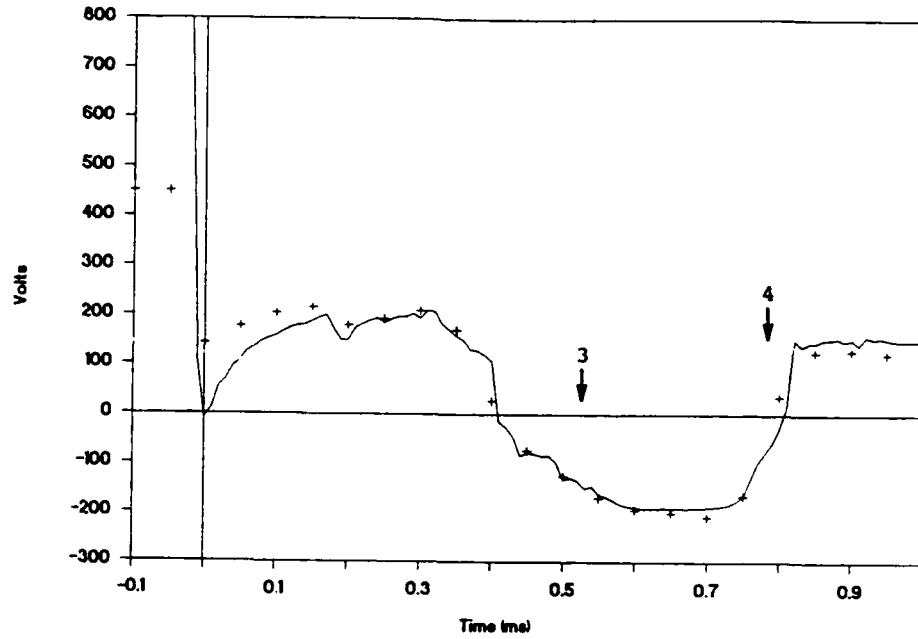


Figure 10. The Plate Voltage.

These results show that the voltage for the first half-cycle (0.0 μs to 410 μs) and the second half-cycle (410 μs to 820 μs) does not depend strongly on the current. The only time the arc voltage changes significantly is when the current passes through zero and reverses direction.

Although the arc voltage (Figure 10) does not display any significant features in the time interval between 530 μs and 790 μs , the electric-field sensor (Figure 9), which responds to the time derivative of the electric field between the plates, clearly shows some features at these times. For example, beginning at 530 μs , when the back end of the wire begins to move away from the ground plate, the time derivative of the voltage starts to increase linearly and generally continues to do so until the wire leaves the hot plate at 790 μs . At this point, the conduction path between the plates no longer contains a segment of copper wire but consists entirely of an arc or arcs. Thus, the electric-field sensor, which as noted earlier actually responds to the time derivative of the electric field between the plates, appears to show some features more clearly than other perhaps more direct ways of determining the plate voltage.

4. SUMMARY

Principal goals of the development effort were twofold: (1) to provide a closing switch simulator (i.e., an external [to the power supply] mechanical means of connecting the power supply to the load); and (2) to provide a spatial region where controllable electric and magnetic fields could be established. Both goals were realized in the present version of the test stand by using an air gun to propel a copper wire through two small holes in an electrified-plate assembly.

Nonintegrating Rogowski coils were developed and used to determine the currents in the LC circuit arrays and between the parallel plates. Good agreement was observed between the measured currents and a circuit theory description of the experiment. In addition, the voltage across the parallel-plate array was inferred from the current measurements and compared with the voltage obtained by integration of a sensor (also developed in the present experiment), which responds to the time derivative of the electric field between the parallel plates. Good, qualitative agreement between the two determinations was obtained although the field sensor did not provide good, quantitative data. The field sensor signal did, however,

display more sensitivity to some of the underlying physical phenomena occurring in the region of the electrical arcs than did the other techniques used to infer the value of the plate voltage. For example, the field sensor clearly indicated plate voltage changes were occurring during a period when the conduction path included a variable-length arc. This effect was not really discernible from the integrated signal (i.e., the plate voltage).

The velocity of the wire was measured by optical means prior to its entry into the electrified-plate region. The value obtained in this fashion was compared to that inferred from oscilloscope traces related to the time interval between a known location of the tip of the wire and time of initial current flow between the plates, the latter indicated by the Rogowski coils. These comparisons showed that the velocity of the wire could be determined to within an error of 3%, which is more than adequate for the planned experiments. At present, a variety of techniques for the early initiation of an arc and, subsequently, current flow between the parallel plates is being studied. Future activities will include using the electrical arcs created in the test stand to develop optical diagnostic techniques to be used in planned range experiments.

Not all of the diagnostics developed here are directly applicable to range experiments. For example, the velocity measurement technique is useful only for the test stand. However, the time resolutions and signal magnitudes for most of the sensors described in this report are, in large part, comparable to those expected in future experiments. More importantly, the test stand provides a convenient facility for the development of new diagnostics and diagnostic techniques as well as a convenient and flexible means for calibration of existing instruments.

5. REFERENCES

- Cobine, J. D. Gaseous Conductors. New York: McGraw-Hill, First edition, p. 348, 1941.
- Johnson, R. F., and A. F. Toepfer. "Disruption of Shaped Charge Jets Using MHD Forces." Final Report from Physics International to FMC, February 1985.
- Littlefield, D. L., and J. D. Powell. "The Effect of Electromagnetic Fields on the Stability of a Uniformly Elongating Plastic Jet." Phys. Fluids A, vol. 2, p. 12, December 1990.
- Lim, M. F., and P. Cayere. "Electromagnetic Armor Proof-of-Principle Test Program." Physics International Draft Report to DNA under Contract DNA001-87-C-01011, January 1988.
- Pellinen, D. G., M. S. DiCapua, S. E. Sampayan, H. Gerbracht, and M. Wang. "Rogowski Coil for Measuring Fast, High-Level Pulsed Currents." Review of Scientific Instruments, vol. 51, p. 1535, 1980.
- Powell, J. D., and D. L. Littlefield. "Effect of Electromagnetic Fields on the Stability of a Perfectly Conducting, Axisymmetric Shaped-Charge Jet." BRL-TR-3108, U. S. Army Ballistic Research Laboratory, Aberdeen Proving Ground, MD, June 1990.
- Walker, E. H. "Defeat of Shaped Charge Devices by Active Armor." BRL-MR-2309, U.S. Army Ballistic Research Laboratory, Aberdeen Proving Ground, MD, July 1973.

INTENTIONALLY LEFT BLANK.

**APPENDIX A:
PHOTO DETECTION SYSTEM CIRCUITRY**

INTENTIONALLY LEFT BLANK.

A particularly simple type of photo-detection system consists of a PIN diode used as a voltage source to directly drive a high input-impedance amplifier. A disadvantage of this kind of detector is that it is relatively insensitive, requiring large light levels to produce voltages significantly above normal laboratory levels of background light and electronic noise. The linearity, response time, and sensitivity for most PIN-diode detection systems can be improved by operating the diode in a reverse-biased mode. The detection system used in the present experiment (Figure A-1) is operated in this mode.

In Figure A-1, resistors R1 and R2, in conjunction with operational amplifier No. 2, form the required reverse-bias network. In the absence of a light signal, the circuit behavior of the photodiode is identical to that of a regular diode (i.e., the current in the forward direction increases rapidly as the amplitude of the forward voltage is increased). When the voltage is in the reverse direction, the diode passes a current, the magnitude of which decreases slightly as the amplitude of the reverse voltage increases. Therefore, to achieve the desired response time and sensitivity, the problem is that of detecting a small current in the presence of a large background PIN diode current and converting this to an adequate voltage signal. The circuit shown in Figure A-1 performs this separation by biasing out the background current.

Consider the three paths that current can take to or from point A in Figure A-1:

(1) through the PIN diode, (2) through the feedback resistor R_2 of operational amplifier Number 1, and (3) through the biasing resistor R_1 . Therefore, the output voltage of the operational amplifier is

$$V_{out} = R_2 (I_{bg} - I_{bias}), \quad (1)$$

where V_{out} is the output voltage of the amplifier, I_{bg} is the background current of the PIN diode which is negative, and I_{bias} is the current through the bias resistor R_1 .

To illustrate how this circuit biases out most of the background current, let the output voltage of the first operational amplifier be applied to the input of the second, a noninverting amplifier with a gain of about 8.0. Actually, there is an RC filter between the output of the first amplifier and the input of the noninverting amplifier; but the input voltage of the latter will be the same as the output voltage of the first amplifier, in a steady state. Thus, the output

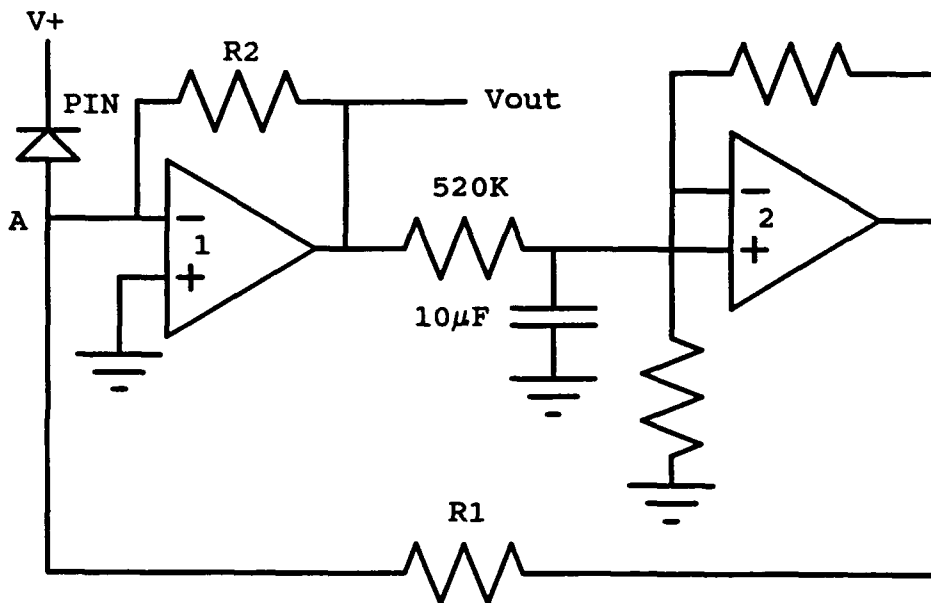


Figure A-1. Self-Biasing PIN Diode Amplifier.

voltage from operational amplifier Number 1 is multiplied by 8 and is applied across the biasing resistor R_1 . The biasing current is then:

$$I_{\text{bias}} = 8.0 V_{\text{out}}/R_1. \quad (2)$$

Eliminating I_{bias} in Equation 1 and Equation 2 and solving for V_{out} the steady-state output voltage is then:

$$V_{\text{out}} = \left[\frac{R_1}{R_1 + 8R_2} \right] R_2 I_{\text{bg}}. \quad (3)$$

The quantity " $R_2 I_{\text{bg}}$ " represents the output voltage that would result in the absence of a bias circuit or current. The term within the brackets thus represents an attenuation of the output signal due to the action of the second amplifier.

It is desirable to operate with circuit parameters which provide a voltage change of several volts when the light beam is interrupted by the arrival of the wire. To illustrate, assume that

the PIN diode is operated with a background current of $0.25 \mu\text{A}$ and the feedback resistor $R_2 = 28\text{M } \Omega$. With no bias, the output voltage would be -7 V . If, however, the biasing circuit shown in Figure 3 is used with $R_1 = 14\text{M } \Omega$, the output voltage is reduced to 0.41 V . Optimum sensitivity would be obtained by selecting a value for R_1 , which reduces the output to zero for the normal background current; however, operating with a small residual value of the voltage provides a useful diagnostic because the output is still proportional to the diode current.

Since the rise time of the output signal introduces an uncertainty in the determination of the position of the wire, this time should be made as small as possible or at least be known. The rise time of the circuit alone was measured by mounting a flashing light emitting diode (LED) close to the PIN diode, before the light pipe was installed. The LED was driven by a pulser with a rise time less than a nanosecond which turned the LED on and off with a rise and fall time on the order of a nanosecond. This produced a pulse at the output of the light pipe amplifiers with a rise and fall time of $0.5 \mu\text{s}$. This resolution was considered to be more than adequate for the present experiments due to the anticipated low velocity of the copper wire.

INTENTIONALLY LEFT BLANK.

**APPENDIX B:
ROGOWSKI COILS FOR CURRENT MEASUREMENTS**

INTENTIONALLY LEFT BLANK.

The output voltage from a Rogowski coil may be required to drive instruments with a limited input voltage range and an input impedance which can alter the apparent response time of the coil. Pellinen et al. (1980) presented a general approach to the design of both self-integrating and non-self-integrating Rogowski coils. To simplify the determination of coil parameters, we make a few assumptions about the expected use of the coil and apply Pellinen's approach. We assume a Rogowski coil, wound on a toroidal form with square cross section, which is used to drive a load with a resistance much larger than the resistance of the coil windings.

The sensitivity of the coil can then be calculated as follows. If a current path is assumed to be on the cylindrical symmetry axis of the coil, then

$$\Phi = I w \mu_0 \ln (R_o/R_i) / 2\pi , \quad (1)$$

where Φ is the magnetic flux inside the toroid, I is the current in the current path, w is the width of the toroid, R_o is the outside radius of the toroid, and R_i is the inside radius of the toroid as shown in Figure B-1. Since

$$V = -N d\Phi/dt = -N w \mu_0 \ln (R_o/R_i) / 2\pi di/dt , \quad (2)$$

where V is the output voltage and N is the number of turns, the sensitivity (S) of the coil is the coefficient of the time derivative of the current, or

$$S = N w \mu_0 \ln (R_o/R_i) / 2\pi . \quad (3)$$

Given an estimate of the expected value of the time derivative of the current, these equations can be used to design a coil to provide the desired voltage output.

If the current in the central conductor could change instantaneously, the output voltage from an ideal coil would be a spike with zero width and infinite voltage. The signal from a practical coil, however, is an exponentially decaying voltage. The time constant for this exponential decay is the response time of the coil and is dependent on the inductance of the

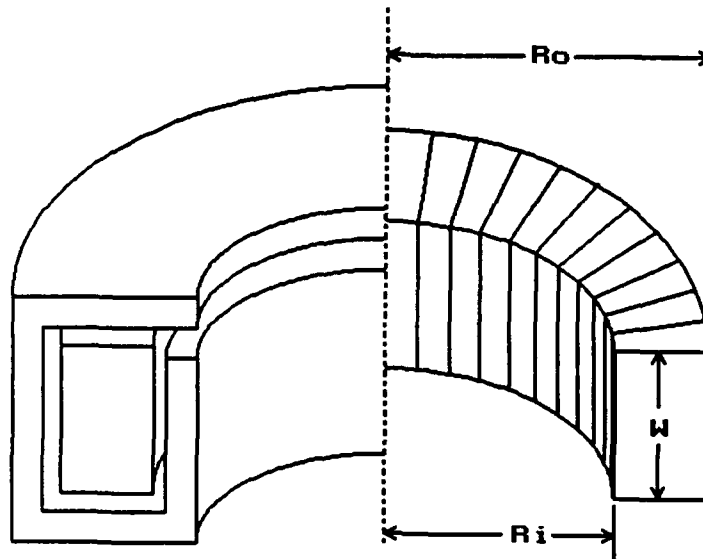


Figure B-1. Rogowski Coil in a Toroidal Housing.

coil and the load resistance. When stray capacitances are ignored and considering the Rogowski coil and the load resistance as a pure LR circuit,

$$\tau = L/R, \quad (4)$$

where τ is the response time of the circuit, R is the load resistance, and L is the inductance of the coil. Since

$$L = N^2 w \mu_0 \ln (R_o/R_i) / 2\pi, \quad (5)$$

then,

$$L = NS. \quad (6)$$

Eliminating the inductance from Equation 7 then,

$$\tau R = NS . \quad (7)$$

Since the time derivative of the expected currents are on the order of 10^8 A/s, the desired sensitivity, S , of the Rogowski coils is $S = 10^{-7}$ V s/A in order to produce a 10-V signal across a 50- Ω load. In addition, the time response should be about 1.0 μ s to satisfy other requirements. Thus, according to Equation 7, the coil should have 500 turns. All of these requirements could not be met with the available materials. It was decided that the sensitivity was the most important consideration and that the requirement on the number of turns was to be met as closely as possible.

A plexiglass tube with an inside diameter of 7.6 cm and an outside diameter of 8.9 cm was used as a coil form to support approximately 349 turns of closely spaced, 22-gauge wire. With these parameters and a sensitivity of 10^{-7} V s/A, the width of the coil (w) should be 0.9 cm (according to Equation 6). The inductance of the coil should then be 34.9 μ H (according to Equation 9) and have a response time of 0.7 μ s (according to Equation 7). Four Rogowski coils were fabricated using these forms, and each Rogowski was encased in a toroidal aluminum housing. Being a conductive loop surrounding the coil, this housing excluded any undesirable axial magnetic fields. A slot in the toroidal housing (giving it a "C" cross section as shown on the left side of Figure B-1) precluded currents whose fields would cancel those linking the windings.

INTENTIONALLY LEFT BLANK.

<u>No. of</u> <u>Copies</u>	<u>Organization</u>	<u>No. of</u> <u>Copies</u>	<u>Organization</u>
2	Administrator Defense Technical Info Center ATTN: DTIC-DDA Cameron Station Alexandria, VA 22304-6145	1	Commander U.S. Army Tank-Automotive Command ATTN: ASQNC-TAC-DIT (Technical Information Center) Warren, MI 48397-5000
1	Commander U.S. Army Materiel Command ATTN: AMCAM 5001 Eisenhower Ave. Alexandria, VA 22333-0001	1	Director U.S. Army TRADOC Analysis Command ATTN: ATRC-WSR White Sands Missile Range, NM 88002-5502
1	Commander U.S. Army Laboratory Command ATTN: AMSLC-DL 2800 Powder Mill Rd. Adelphi, MD 20783-1145	1	Commandant U.S. Army Field Artillery School ATTN: ATSF-CSI Ft. Sill, OK 73503-5000
2	Commander U.S. Army Armament Research, Development, and Engineering Center ATTN: SMCAR-IMI-I Picatinny Arsenal, NJ 07806-5000	2	Commandant U.S. Army Infantry School ATTN: ATZB-SC, System Safety Fort Benning, GA 31903-5000
2	Commander U.S. Army Armament Research, Development, and Engineering Center ATTN: SMCAR-TDC Picatinny Arsenal, NJ 07806-5000	(Class. only)1	Commandant U.S. Army Infantry School ATTN: ATSH-CD (Security Mgr.) Fort Benning, GA 31905-5660
1	Director Benet Weapons Laboratory U.S. Army Armament Research, Development, and Engineering Center ATTN: SMCAR-CCB-TL Watervliet, NY 12189-4050	(Unclass. only)1	Commandant U.S. Army Infantry School ATTN: ATSH-CD-CSO-OR Fort Benning, GA 31905-5660
(Unclass. only)1	Commander U.S. Army Rock Island Arsenal ATTN: SMCRI-TL/Technical Library Rock Island, IL 61299-5000	1	WL/MNOI Eglin AFB, FL 32542-5000 <u>Aberdeen Proving Ground</u>
1	Director U.S. Army Aviation Research and Technology Activity ATTN: SAVRT-R (Library) M/S 219-3 Ames Research Center Moffett Field, CA 94035-1000	2	Dir, USAMSAA ATTN: AMXSY-D AMXSY-MP, H. Cohen
1	Commander U.S. Army Missile Command ATTN: AMSMI-RD-CS-R (DOC) Redstone Arsenal, AL 35898-5010	1	Cdr, USATECOM ATTN: AMSTE-TC
		3	Cdr, CRDEC, AMCCOM ATTN: SMCCR-RSP-A SMCCR-MU SMCCR-MSI
		1	Dir, VLAMO ATTN: AMSLC-VL-D
		10	Dir, USABRL ATTN: SLCBR-DD-T

No. of
Copies Organization

- 1 Director
Defense Advanced Research
Projects Agency
ATTN: Dr. Peter Kemmey
1400 Wilson Blvd.
Arlington, VA 22209
- 1 Commander
SDIO
ATTN: SDIO/IST,
MAJ M. Huebschman
Washington, DC 20301-7100
- 5 Commander
U.S. Army Armament Research,
Development, and Engineering Center
ATTN: SMCAR-FSA-E,
Dr. T. Gora
John Bennett
SMCAR-AEE-B,
Dr. D. Downs
SMCAR-CCL-FA,
H. Moore
H. Kahn
Picatinny Arsenal, NJ 07606-5000
- 2 Director
Benet Weapons Laboratory
U.S. Army Armament Research,
Development, and Engineering Center
ATTN: SMCAR-CCB-DS,
Dr. C. A. Andrade
SMCAR-CCB-RM,
Dr. Pat Vottis
Watervliet, NY 12189
- 1 Director
U.S. Army Research Office
ATTN: Dr. Michael Ciftan
P. O. Box 12211
Research Triangle Park, NC 27709-2211
- 2 Commander
U.S. Army Electronics Technology and
Devices Laboratory
Pulse Power Technology Branch
ATTN: SLCET-ML, Dr. Thomas Podlesak
SLCAT-P, Dr. Hardev Singh
Fort Monmouth, NJ 07703

No. of
Copies Organization

- 1 Commander
U.S. Navy David Taylor Research Center
Code 1740.3
ATTN: Dr. Ray Garrison
Bethesda, MD 20084
- 4 CG, MCRDAC
Code AWT
ATTN: Dr. C. Vaughn
Mr. C. Childers
MAJ R. Jensen
Mr. G. Solhand
Quantico, VA 22134-5080
- 2 Air Force Armament Laboratory
ATTN: AFATL/DLJG,
Mr. Kenneth Cobb
AFATL/DLDG,
Dr. T. Aden
Eglin AFB, FL 32542-5000
- 1 Director
Brookhaven National Laboratory
ATTN: Dr. J. R. Powell
Bldg 129
Upton, NY 11973
- 1 Director
Lawrence Livermore National Laboratory
ATTN: Dr. R. S. Hawke, L-156
P. O. Box 808
Livermore, CA 94550
- 3 Director
Los Alamos National Laboratory
ATTN: MSG 787,
Mr. Max Fowler
Dr. J. V. Parker
Dr. William Condit
Los Alamos, NM 87545
- 1 Sandia National Laboratory
ATTN: Dr. Maynard Cowan
Dept. 1220
P. O. Box 5800
Albuquerque, NM 87185

<u>No. of</u> <u>Copies</u>	<u>Organization</u>
1	NASA Lewis Research Center ATTN: MS 501-7, Lynette Zana 2100 Brook Park Road Cleveland, OH 44135
2	Auburn University ATTN: Dr. Raymond F. Askew, Leach Nuclear Science Center Dr. E. J. Clothiaux, Department of Physics Auburn University, AL 36849-3501
1	Texas Technical University Department of EE/Computer Science ATTN: Dr. M. Kristiansen Lubbock, TX 79409-4439
1	Tuskegee Institute Dept. of Mechanical Engineering ATTN: Dr. Pradosh Ray Tuskegee Institute, AL 36088
1	University of Alabama in Huntsville School of Science & Engineering ATTN: Dr. C. H. Chen Huntsville, AL 35899
1	University of Miami ATTN: Dr. Manuel A. Huerta, Physics Dept. P.O. Box 248046 Coral Gables, FL 33124
1	University of Tennessee Space Institute ATTN: Dr. Dennis Keefer Tullahoma, TN 37388-8897
3	University of Texas Center for Electromechanics Balcones Research Center ATTN: Mr. William Weldon Mr. Raymond Zaworka 10100 Burnet Road, Bldg. 133 Austin, TX 78748

<u>No. of</u> <u>Copies</u>	<u>Organization</u>
1	University of Texas at Austin Institute for Advanced Technology ATTN: Dr. Harry Fair 1011 Burnet Rd. Austin, TX 78758
1	Astron Research & Engineering ATTN: Dr. Charles Powars 130 Kifer Court Sunnyvale, CA 94086
2	Austin Research Associates ATTN: Dr. Millard L. Sloan Dr. William E. Drummond 1091 Rutland Drive Austin, TX 78758
3	Maxwell Laboratories ATTN: Dr. Rolf Dethlefsen Dr. Ian McNab Dr. Mark Wilkinson 8888 Balboa Avenue San Diego, CA 92123
1	California Research and Technology, Inc. Titan Technologies ATTN: Dr. Richard F. Johnson 20943 Devonshire Street Chatsworth, CA 91311-2376
1	Titan Technologies ATTN: Dr. R. B. Miller P.O. Box 4399 Albuquerque, NM 87196
1	Boeing Aerospace Company ATTN: Dr. J. E. Shrader P. O. Box 3999 Seattle, WA 98134
2	GA Technologies, Inc. ATTN: Dr. Robert Bourque Dr. L. Holland P. O. Box 85608 San Diego, CA 92138

**No. of
Copies** **Organization**

1 General Dynamics
ATTN: Dr. Jaime Cuadros
P. O. Box 2507
Pomona, CA 91766

2 Electromagnetic Research, Inc.
ATTN: Dr. Henry Kolm
Dr. Peter Mongeau
2 Fox Road
Hudson, MA 01749

2 General Electric Company (AEPD)
ATTN: Dr. William Bird
Dr. Slade L. Carr
R. D. #3, Plains Road
Ballston Spa, NY 12020

1 General Research Corporation
ATTN: Dr. William Isbell
P. O. Box 6770
Santa Barbara, CA 93160-6770

2 IAP Research, Inc.
ATTN: Dr. John P. Barber
Mr. David P. Bauer
2763 Culver Avenue
Dayton, OH 45429-3723

2 LTV Aerospace & Defense Company
ATTN: MS TH-83,
Dr. Michael M. Tower
Dr. C. H. Haight
P. O. Box 650003
Dallas, TX 75265-0003

1 Pacific-Sierra Research Corp.
ATTN: Dr. Gene E. McClellan
1401 Wilson Blvd.
Arlington, VA 22209

1 R&D Associates
ATTN: Dr. Peter Turchi
P.O. Box 9695
Marina del Rey, CA 90291

1 Science Applications International Corporation
ATTN: Dr. K. A. Jamison
1247-B North Eglin Parkway
Shalimar, FL 32579

**No. of
Copies** **Organization**

3 Science Applications International Corporation
ATTN: Dr. Jad H. Batteh
Dr. G. Rolader
Mr. L. Thornhill
1503 Johnson Ferry Road, Suite 100
Marietta, GA 30062

1 System Planning Corporation
ATTN: Donald E. Shaw
1500 Wilson Blvd.
Arlington, VA 22209

1 Westinghouse Electric Corporation
Marine Division
ATTN: Dr. Dan Omry
401 East Hendy Avenue
Sunnyvale, CA 94088-3499

2 Westinghouse Science and Technology
Center
ATTN: Dr. Bruce Swanson
Mr. Doug Fikse
1310 Beulah Road
Pittsburgh, PA 15233

2 SPARTA Inc.
ATTN: Jeffery Kezerian
Dr. Michael M. Holland
9455 Towne Centre Drive
San Diego, CA 92121-1964

1 Supercon Inc.
ATTN: Charles Renaud
830 Boston Turnpike Road
Shrewsbury, MA 01545

Aberdeen Proving Ground

1 Cdr, USATECOM
ATTN: AMSTE-SI-F

USER EVALUATION SHEET/CHANGE OF ADDRESS

This laboratory undertakes a continuing effort to improve the quality of the reports it publishes. Your comments/answers below will aid us in our efforts.

1. Does this report satisfy a need? (Comment on purpose, related project, or other area of interest for which the report will be used.) _____

2. How, specifically, is the report being used? (Information source, design data, procedure, source of ideas, etc.) _____

3. Has the information in this report led to any quantitative savings as far as man-hours or dollars saved, operating costs avoided, or efficiencies achieved, etc? If so, please elaborate. _____

4. General Comments. What do you think should be changed to improve future reports? (Indicate changes to organization, technical content, format, etc.) _____

BRL Report Number BRL-TR-3358 Division Symbol _____

Check here if desire to be removed from distribution list. _____

Check here for address change. _____

Current address: Organization _____
Address _____

DEPARTMENT OF THE ARMY
Director
U.S. Army Ballistic Research Laboratory
ATTN: SLCBR-DD-T
Aberdeen Proving Ground, MD 21005-5066



NO POSTAGE
NECESSARY
IF MAILED
IN THE
UNITED STATES

OFFICIAL BUSINESS

BUSINESS REPLY MAIL
FIRST CLASS PERMIT No 0001, AFG, MD

Postage will be paid by addressee.

Director
U.S. Army Ballistic Research Laboratory
ATTN: SLCBR-DD-T
Aberdeen Proving Ground, MD 21005-5066

